Journal of the Korean Physical Society, Vol. 51, July 2007, pp. S42∼S46

Numerical and Experimental Analysis of Electrostatic Ejection of Liquid Droplets

Yong-Jae Kim and Han Seo Ko*
School of Mechanical Engineering, Sungkyunkwan University, Suwon 440-746

Sukhan Lee, Sang Uk Son and Daewon Jung
School of Information and Communication Engineering, Sungkyunkwan University, Suwon 440-746

Doyoung Byun
School of Mechanical and Aerospace Engineering, Konkuk University, Seoul 143-701

An electrostatic inkjet head can be used for processes of manufacture of large display systems and printed circuit boards (PCB), as well as inkjet printers, because an electrostatic field provides an external force which can be manipulated to control sizes of droplets. The existing printing devices such as thermal bubble and piezo inkjet heads have shown difficulties in controlling the ejection of the droplets for printing applications. Thus, a new inkjet head using electrostatic force is proposed in this study. In order to prove the theory of the developed electrostatic inkjet head, the applicable and basic theory has been studied by using distilled water and water with sodium dodecyl sulfate (SDS). Also, a numerical analysis has been performed to calculate the intensity of the electrostatic field by using Maxwell's equation. Furthermore, experiments have been carried out by using a downward glass capillary with an outside diameter of 500 μm. Gravity, surface tension, and electrostatic force have been analyzed with voltages of 0 to 5 kV. It has been observed that the droplet size decreases and the frequency of droplet formation and the velocity of droplet ejection increase with increasing intensity of the electrostatic field. The results of the experiments have shown good agreement with those of numerical analysis.

PACS numbers: 47.55.D, 47.55.DM, 47.65.D
Keywords: Electrostatic, Droplet, Inkjet, Ejection

I. INTRODUCTION

There has been a tremendous increase in the use of micro droplets in physical, chemical, biological and engineering research areas such as micro-detectors, combinatorial chemistry assays using high cost chemicals, and micro-dispensing of small sub-nanoliter volumes of fluids for sensors, flat panel displays, and biochips [1–4]. Since the conventional jetting devices based on thermal bubble or piezoelectric pumping have some fundamental limitations on the density of the nozzle array as well as the ejection frequency, electrostatic jetting based on the direct manipulation of liquid by an electric field appears to be more promising [5].

Experimental and theoretical investigations on the electro-spraying of liquids have been performed by many researchers. Scaling laws of spray were presented by using liquids with different viscosities, surface tension, electrical conductivities, and permittivity [6]. Sato *et al.* [7] measured the surface tension of liquid under applied D.C. electric field and concluded that the surface tension decreased with increasing voltage and the reduction was proportional to the square of the field strength. Uniformly sized droplets less than several micrometers in diameter have been produced by Vonnegut *et al.* [8] by using positive voltage applied to nozzle electrodes in air. They carried out experiments using aqueous electrolyte solution by varying the water conductivity and derived an equation to estimate the formed droplet sizes as a function of flow rate, surface tension, and electrical charge. They concluded that electrostatic jetting occurred by an electrical constriction force acting on a liquid meniscus.

A novel mechanism of electrostatic micro droplet formation and ejection of fluid is proposed in this study. The detailed jetting mechanisms and modes have been investigated to design the electrostatic jetting system optimally and to examine forces on the jetting mechanism for droplet-on-demand operation according to important physical parameters such as surface tension, which is reduced by electrical conductivity of liquid due to applied voltages.

*E-mail: hanseoko@yurim.skku.ac.kr

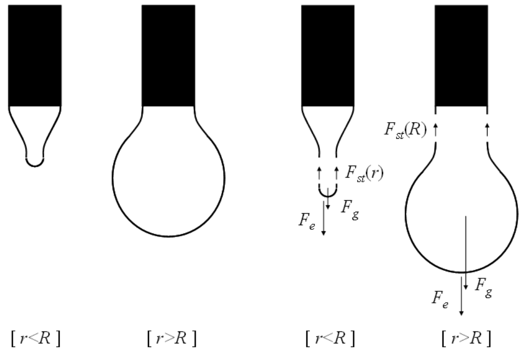

Fig. 1. Main forces acting on droplet.

A micro-dripping mode is the optimum method for ejection of liquid for droplet-on-demand operation among a number of spraying modes which depend on many parameters such as applied voltages, liquid flow rates, and physical properties, as well as electric field strength and configuration [9]. Thus, it is hard to search the suitable range for liquid ejection in micro-dripping mode by controlling various parameters. In this study, the change of droplet size has been observed according to the force for the droplet formation, instead of the physical properties of the liquid. Also, equations have been derived for the various forces, to compare with the experimental results.

II. NUMERICAL ANALYSIS

A simple model to predict the droplet diameter in the dripping mode has been derived by Speranza *et al.* with measurements of droplet sizes and formation frequencies for highly conductive and viscous liquids [7,8]. However, the model of Speranza has shown discrepancies with the experimental results for an electric field higher than 106 V/m. The reduced amount of the droplet size increased with increasing applied voltage in the experimental results, while it decreased with the derived model. Thus, a more accurate model is proposed in this study considering the surface-tension reduction which has not been included in previous research, and this is confirmed by the experimental results.

Former researchers have indicated that the process of dripping is essentially quasi-static in nature, with negligible inertial and viscous effects of the fluid flow [10,11]. Therefore, a simple static force balance can be applied at all stages of the droplet formation, from which the droplet diameter can be expressed as a function of the applied electric force [12].

The forces taken into account in the force balance are F_g due to gravity, F_{st} due to surface tension, and F_e due to the electric field (Figure 1). The following equation can be derived for the force balance:

$$F_g - F_{st} + F_e = 0 \ . \tag{1}$$

The electrostatic force acting on the pendant drop is related to the geometry of the electrode, which provides a nonuniform electric field. The electric field due to a potential applied to a semi-infinite wire with a rounded end and an infinite plate configuration [13] has been modified in this study as follows:

$$E = \frac{\sqrt{2}V}{r'\ln\left(\frac{4D'}{r'}\right)} \ , \tag{2}$$

where r' is the modified radius of the droplet for the electric field, V is the electric potential, and D' is the modified distance between the wire end and the earthed electrode. The results for the three-dimensional electric field from the numerical analysis at the instant of droplet formation have varied with the radius of curvature at the surface of the liquid. Thus, the electric field depends on the radius of the formed droplet, because the radius of curvature at the surface of the liquid is very similar to the radius of the droplet. Eq. (3) has been derived to consider this phenomenon:

$$r' = \begin{cases} K_1(r-R)+R, & r \le R \\ K_2(r-R)+R, & r > R \end{cases} \ , \tag{3}$$

where r is the radius of the droplet, r' is the modified radius of the droplet, R is the radius of the wire end, and K is the correction factor for the radius of the droplet, with K_1 of 0.95 and K_2 of 1.2. Also, the distance between the wire end and the earthed electrode is a very important factor for the electric field intensity at the instant of droplet formation. If the droplet size increases, the distance decreases when forming the droplet. Thus, Eq. (4) has been included in Eq. (2):

$$D' = D - 2r \ , \tag{4}$$

where D is the distance between the wire end and the earthed electrode and D' is the modified distance for D. It has been confirmed by computational analysis that the electric field intensity is affected by the radius of the droplet, as well as the radius of the wire end. Thus, the correction factor K has been introduced to obtain the electric field intensity considering both sizes. Because of the difference of the distribution of the electric field as shown in Figure 2, the use of K has been divided into droplet diameter > capillary diameter and droplet diameter < capillary diameter. The electric field has the same direction as the droplet ejection (Figure 2 (a)), while the opposite direction of the distribution of the electric field (Figure 2 (b)) weakens for the electrostatic force for droplet ejection. Thus, the equations (Eqs. (3) and (4)) have been derived to calculate the electric field and they have shown good agreement with the results of the computer simulation as shown in Figure 3.

The electrostatic force with the electric field acting on the pendant droplet can be evaluated in the following way:

$$F_e = \frac{1}{2}S\varepsilon_o E^2 \ , \tag{5}$$

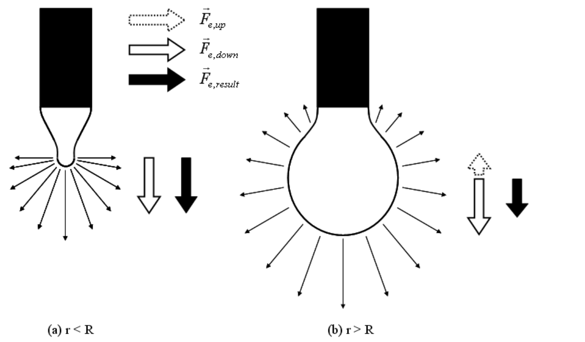

Fig. 2. Electrostatic force caused by distribution of electric field around meniscus of liquid.

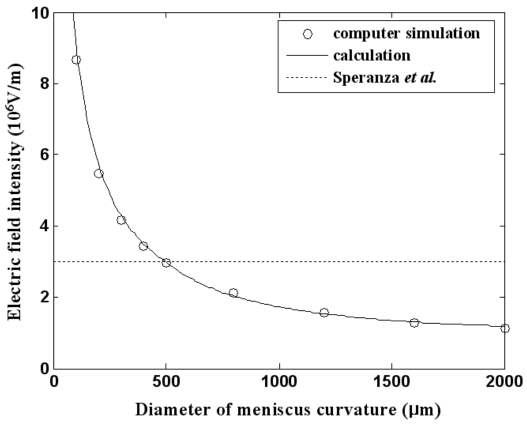

Fig. 3. Electric field intensity with diameters of droplets.

where S is the surface area of the drop and ε_o is the permittivity of air [14]. According to Takamatsu *et al.* [15], the electrostatic force acting on the pendant drop can be considered to be equivalent to the electrostatic force acting on the formed drop, with a small margin of error. Also, the drop is considered to have a spherical shape, ignoring any deformation of the surface induced by the action of the electrostatic force [16]. The force due to the surface tension can be obtained as follows:

$$F_{st} = \begin{cases} f(2\pi r)\gamma, & r \le R \\ f(2\pi R)\gamma, & r > R \end{cases}, \tag{6}$$

$$\gamma = \gamma_o \left(1 - \frac{V^2}{V_{ref}^2}\right), \tag{7}$$

where γ is the surface-tension constant with the applied voltage, γ_o is the surface-tension constant without the applied voltage, f is the Harkins correction factor for the range of the considered droplet diameter, with the value of 0.65 [17], and V_{ref} is the reference value of the applied voltage. The assumption of f allows an error below 10 % for the analytical result in the evaluation of the force due to the surface tension. The surface tension is proportional to the droplet size if the droplet diameter is smaller than the capillary diameter; otherwise, it depends on the capillary diameter (Eq. (6)). The surface tension also decreases with increasing applied voltage, and the reduction is proportional to the square of the applied field strength [7, 18]. Thus, Eq. (7) has been derived to calculate the surface tension with the applied voltage, as shown in Figure 4. The gravitational force F_g, which is related to the droplet mass, can be written as follows:

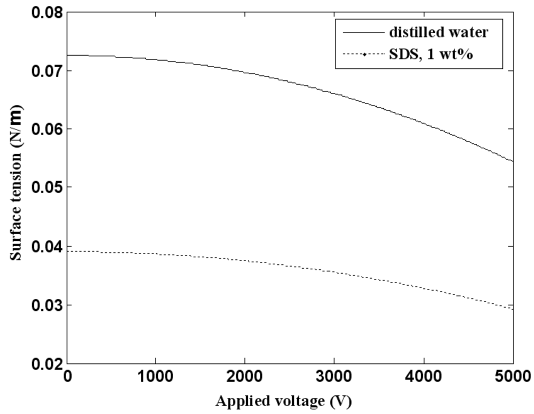

Fig. 4. Surface tension with applied voltage.

$$F_g = \left(\frac{4}{3}\pi r^3\right)\rho g, \tag{8}$$

where ρ is the droplet density and g is the gravitational acceleration.

The droplet radius r is the variable for all terms of the gravitational force, the surface tension, and the electrostatic force, as shown by Eqs. (2) to (8). Therefore, the trial and error method has been used to calculate the droplet radius r in the state of balance of the three forces, which are also affected by the droplet radius.

III. EXPERIMENTAL SETUP

A droplet is formed and ejected by a pair of electroplates with a hole (5 mm) at the center and a micro glass capillary tube with an outside diameter of 500 μm including a pole made of Pt wire, as shown in Figure 5. Images of droplet ejection (Figure 6) were captured by a high-speed camera (IDT XS-4) at 5000 frames a second and 512 × 512 pixel resolution with a micro-zoom lens (infinity K2), and a 100-W halogen lamp. A high-voltage power supply system with maximum voltage of 5.0 kV was used to control the electrostatic field. Liquids were supplied into the glass capillary by a micro-syringe pump. Table 1 shows the properties of the liquids used in this experiment.

The gravitational force is not so significant in this experiment, because the sizes of the capillary and the formed droplet are small. Thus, the main forces including the surface tension and the electrostatic force were

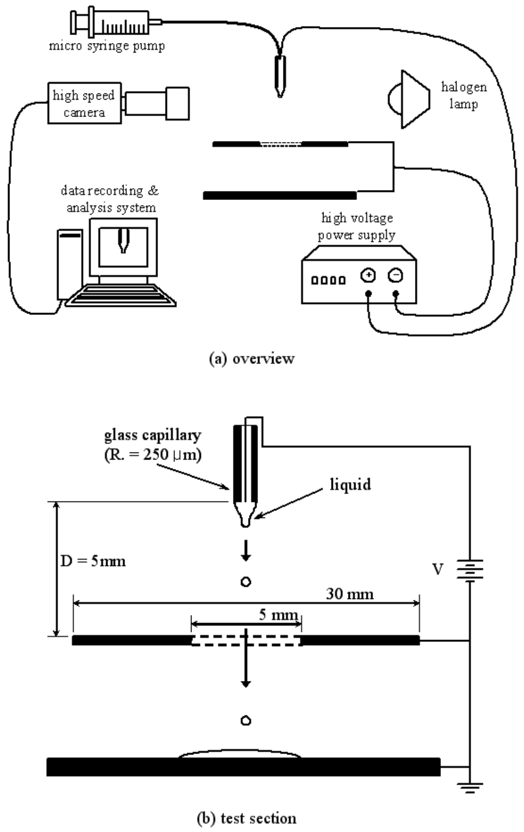

Fig. 5. Experimental setup.

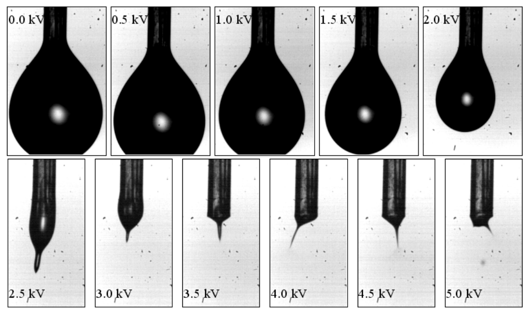

Fig. 6. Meniscus of 1 wt% SDS with droplet formation for various applied voltages.

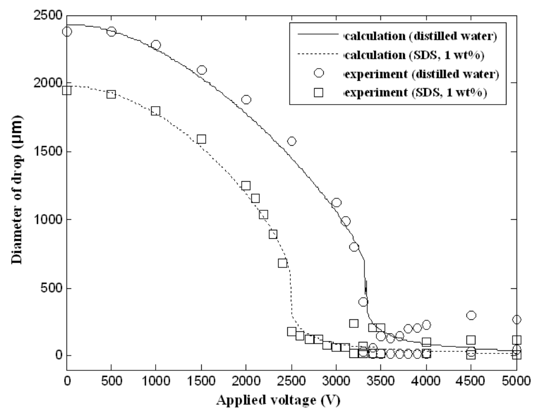

Fig. 7. Distribution of droplet size with applied voltage.

Table 1. Liquid properties.

Liquid	Density [kg/m^3]	Surface tension [N/m]	Electrical conductivity[S/cm]
distilled water	998	0.0725	1.0580×10^{-5}
distilled water + SDS, 1 wt%	1000	0.039	3.8676×10^{-4}

observed with voltages of 0 to 5 kV, and distilled water and water mixed with sodium dodecyl sulfate (SDS), which is a surfactant, were used to investigate the effect of surface tension, because water with SDS has similar density and different surface tension, compared with distilled water.

IV. RESULTS AND DISCUSSION

The liquids were supplied to the micro-capillary with a constant velocity of 10 μl/min by the micro-syringe pump, and voltage was supplied to the electrodes. When the voltage increases, the droplet size decreases and the reduction rate increases, as shown in Figure 7, because the electrostatic force increases and the surface tension decreases to reduce the droplet size for the balance of both forces. Initially, a uniform droplet size appeared with a regular formation frequency for stable ejection, up to 3.3 kV for distilled water. The droplet size then decreased rapidly and the ejection became unstable with irregular frequency and various droplet sizes, 10 μm to 400 μm, from 3.3 kV to 5 kV, since the ejection frequency of the droplet became shorter than the relaxation time of the liquid, so as to make the charge for the liquid unstable. The largest and smallest values for the observed droplets at the same voltage have been shown in the graph of Figure 7. The observed droplets have sizes of 5 to 200 μm for distilled water and 5 to 80 μm for water with 1 wt% SDS in the range between 3.3 kV and 5 kV.

A similar phenomenon to that with distilled water occurred for 1 wt% SDS up to 2.5 kV. However, the droplet size did not vary at the same voltage after 2.5 kV for stable droplet formation in the micro-dripping mode although the droplet size decreased significantly with increasing voltage. A similar phenomenon to that with distilled water after 3.3 kV was observed for 1 wt% SDS at 3.2 kV, showing various droplet sizes. A spindle and oscillating mode and a multi-jet mode appeared for the 1 wt% SDS at 3.5 $\sim$ 4 kV and 5 kV, respectively, as shown in Figures 6 and 7.

The model derived in this study shows good agreement with the experimental results for distilled water and 1 wt% SDS before the unstable ejection (Figure 7), compared with the previous studies, which did not express the great reduction of the droplet size appropriately for the range of high voltages, because the proposed model has used variables for constant surface tension and various electric field intensities. Thus, it has been realized that the prediction of accurate electric field and surface tension is very important for electrostatic ejection of the droplet. Additional experiments and analyses are required in order to investigate the irregular and unstable ejection phenomena for the region of high voltages.

V. CONCLUSION

A new model considering the change of electric field and surface tension has been derived and confirmed by experimental results in this study, to overcome the inaccuracies of the previous studies. Distilled water and 1 wt% SDS have been used to construct the model for the analysis of electrostatic ejection of the droplet. The results of the proposed model show good agreement with the experimental results in calculating accurate sizes of the formed droplets. More experiments and analyses are required in order to optimize the constants applicable to the acting forces, especially for the irregular ejection which has been observed in this study.

ACKNOWLEDGMENTS

This work was supported by Korea Research Foundation Grant funded by the Korean Government (MOEHRD) (KRF-2005-D00045 (I01474)).

REFERENCES

[1] C. M. Ho, in *Proceedings of the IEEE International Conference on MEMS* (Interlaken, 2001), p. 375.
[2] Y. S. Choi and D. H. Park, J. Korean Phys. Soc. **44**, 1556 (2004).
[3] D. J. Seo, J. Korean Phys. Soc. **45**, 1575 (2004).
[4] Y. S. Choi and D. H. Park, J. Korean Phys. Soc. **46**, 1445 (2005).
[5] S. H. Lee, D. Y. Byun, H. S. Ko, Y. J. Kim, J. H. Yang, S. J. Han, S. U. Son and J. T. Oh, in *Proceedings of 2005 NSTI Nanotechnology Conference and Trade Show*, Vol. 1 (Anaheim, 2005), p. 656.
[6] A. M. Ganan-Calvo, J. Davila and A. Barrero, J. Aerosol Sci. **28**, 249 (1997).
[7] M. Sato, M. Kito and T. Sakai, Kagaku Kogaku Ronbunshu **3**, 504 (1977).
[8] B. Vonnegut and R. L. Neubauer, J. Colloid Interface Sci. **7**, 616 (1952).
[9] J. M. Grace and J. C. M. Marijnissen, J. Aerosol Sci. **25**, 1005 (1994).
[10] A. Speranza, M. Ghadiri, M. Newman, L. Sesti Osseo and G. Ferrari, J. Electrostatics **51-52**, 494 (2001).
[11] G. F. Scheele and B. J. Meister, AIChE J. **14**, 9 (1968).
[12] A. Speranza and M. Ghadiri, Powder Tech. **135-136**, 361 (2003).
[13] D. P. H. Smith, IEEE Trans. Ind. Appl. **22**, 527 (1986).
[14] W. J. Duffin, *Electricity and Magnetism* (McGraw-Hill, London, 1973).
[15] T. Takamatsu, M. Yamaguchi and T. Katayama, J. Chem. Eng. of Japan **16**, 267 (1983).
[16] C. H. Byers and J. J. Perona, AIChE J. **34**, 1577 (1988).
[17] A. W. Adamson, *Physical Chemistry of Surfaces* (Wiley, New York, 1990), p. 22.
[18] M. Sato, N. Kudo and M. Saito, IEEE Trans. Ind. Appl. **34**, 294 (1998).
[19] S. B. Norina, S. H. Park and K. S. Soh, J. Korean Phys. Soc. **47**, 297 (2005).